 doi:10.20944/preprints201702.0037.v1

Review

Theranostic Probes for Targeting Tumor Microenvironment: An Overview

Musafar Gani Sikkandhar [1], Anu Maashaa Nedumaran [1], Roopa Ravichandar [1], Satnam Singh [1], Induja Santhakumar [1], Zheng Cong Goh [1], Sachin Mishra [1], Govindaraju Archunan [2], Balázs Gulyás [1,*] and Parasuraman Padmanabhan [1,*]

[1] Lee Kong Chian School of Medicine, Nanyang Technological University, 59 Nanyang Drive, Singapore 636921, Singapore; musafargani030495@gmail.com (M.G.S.); mnmaashaa@gmail.com (A.M.N.); rupsravi@gmail.com (R.R.); saabsatnam01@gmail.com (S.S.); indup1893@gmail.com (I.S.); zgoh009@e.ntu.edu.sg (Z.C.G.); sachin.mishra@ntu.edu.sg (S.M.)

[2] Centre for Pheromone Technology, Department of Animal Science, Bharathidasan University, Tiruchirappalli 620024, India; archunan@bdu.ac.in,

* Correspondence: balazs.gulyas@ntu.edu.sg (B.G.); ppadmanabhan@ntu.edu.sg (P.P.); Tel.: +65-6904-1184 (B.G.); +65-6904-1186 (P.P.); Fax: +65-6515-0417 (B.G.); +65-6515-0417 (P.P.)

Abstract: Long gone was the time when tumors were thought to be insular masses of cells, residing independently at specific sites in an organ. Now, researchers gradually realize that tumors interact with the extracellular matrix (ECM), blood vessels, connective tissues and immune cells in their environment, which is now known as the tumor microenvironment (TME). It is found that the interactions between tumors and their surrounding promote tumor growth, invasion and metastasis. The dynamics and diversity of TME cause the tumors to be heterogeneous and thus pose a challenge for cancer diagnosis, drug design and therapy. As TME is significant in enhancing tumor progression, it is vital to identify the different components in the TME. This review explores how different factors in the TME supply tumors with the required growth factors and signaling molecules to proliferate, invade and metastasis. We also examine the development of TME-targeted nanotheranostics over the recent years for cancer therapy, diagnosis and anticancer drug delivery system. This review further discusses the limitations and future perspective of nanoparticle based theranostics when used in combination with current imaging modalities like Optical Imaging, Magnetic Resonance Imaging (MRI) and Nuclear Imaging (PET and SPECT).

Keywords: tumor microenvironment; nanoparticle; nanotheronostics; probe; imaging

1. Introduction

Cancer is no longer a defect in the cell cycle control due to reasons ranging from external radiation exposure to hereditary gene or a combination of both. Recent advancements in finding the factors that influence cancer development has resulted in the conclusion that even the immediate environment of the cancer cells influences its proliferation. Cancer microenvironment or also known as tumor microenvironment (TME) is an environment in the cellular level, which consists of surrounding cells such as immune cells, inflammatory cells, extracellular matrix and also the physical factors such as the pH, temperature etc. [1]. TME became the topic of interest for many researchers upon the discovery of effect of the immediate environmental changes such as lowering of pH, increased temperature etc. on the proliferation of cancer cells. The contribution of TME is still under research and recent studies suggest that both biochemical and physical cues in the environment significantly affects the growth and development of the cancer cells [2].

One of the predominantly preferred methods to study and understand TME is molecular or metabolic imaging. Recent improvements in the imaging field have greatly impacted the way in which TME is deciphered and has also improved the efficiency to monitor the dynamic interactions between the tumor cells and its surrounding factors. The majority of the probes specialized for TME

 doi:10.20944/preprints201702.0037.v1

target the stromal cells, low oxygen or the hypoxia state and low pH in the TME and the interstitial pressure [3]. With this knowledge, therapy for cancer is developed, known as image guided therapy (IGT) that helps the users monitor the pathway and the function of the probe which is injected into the patient for theranostic purposes. IGT had been around in the medical field and it had been explored significantly. It is mainly used to track the pathway of the imaging probes, detect the progress of drug accumulation in the cells or even externally activate the specific nanoprobe with external factors such as ultrasound, temperature etc. [4]. Although it is almost a well-established technique, there is still room for improvement in the IGT used in computer assisted surgery (CAS) as their abilities are still limited [5].

Imaging is also used during the cancer surgery and this is known as intra-operative imaging. This assists the doctors efficiently, especially during key-hole or laparoscopic surgery to view the inner body image and to monitor the surgery [6]. Thus, optical imaging proves to be a powerful tool for intra-operative imaging due to its high sensitivity and specificity, guiding the doctors to perform precise procedures. This in turn increases the cancer patients' survival rates. Another way of monitoring is using nanotheranostic techniques whereby probes in nanoscale are injected into the body [7]. These probes have specific drugs and target locators engraved or attached to them, contributing to the specificity of the probe. This has proven to be an efficient method to target the TME factors such as pH, temperature etc. The futuristic vision of this technique is to improve the personalized medicine concept, which is to customize the medical procedures to suit the patient's requirements.

One of the most widely used tools in nanotheranostics is nanoparticles (NPs). They come in various types, shapes and sizes according to the target location, the pathway and the application. Each target has a few specific requirements that need to be satisfied by the particular NP, so that the theranostic drug delivery system is efficient. Three main aspects that need to be clarified before choosing a type of NP are: firstly, the knowledge of the target cells and the biomarkers present in that target. The pathway taken by the probe is the next thing to be considered, that is, whether an oral administration or an intra venous (IV) injection etc. Finally, we have to consider the ability of the NP to survive the chosen pathway. For example, we need to consider whether the IV administered nanoprobe can survive the blood circulation and attack from the immune cells till it is absorbed by the targeted cells. Using these guidelines to choose nanoprobes, many available nanomaterials have been designed like nanodots, quantum dots, nanotubes, nanowells etc. As far TME as is considered, most of the probes used are spherical and the trend of polymer-based NPs targeting TME is booming. NPs are proven to be a useful technique for both early detection and drug delivery for cancer cells. For example, Matrix metalloproteinase (MMP-2) responsive nanoprobe is a type of NP developed specifically to target the breast, colon, and prostate cancer cells and to study the role of MMP in promoting cancer progression. This technique was developed to image and analyze the accumulation of macrophages in the cancerous organs [8]. Amongst the discussed nanoprobes, the most suitable ones for MRI scan are iron oxide and gold NPs [9–11].

Most NPs either target the receptors on the cell itself (like p53 targeting probes) or the intracellular trace elements (like zinc in pancreatic beta cells) or the environmental factors specific to the cellular microenvironment (like low pH surrounding cancer cells) [12]. This review aims to summarize TME-specific nanotheranostic probes that have been developed in the past few years designed for different imaging modalities, coupled with their usefulness and limitations. **Figure 1** shows the illustration of theranostic probe incorporated for targeting tumor microenvironment.

Preprints (www.preprints.org) | NOT PEER-REVIEWED | Posted: 13 February 2017 doi:10.20944/preprints201702.0037.v1

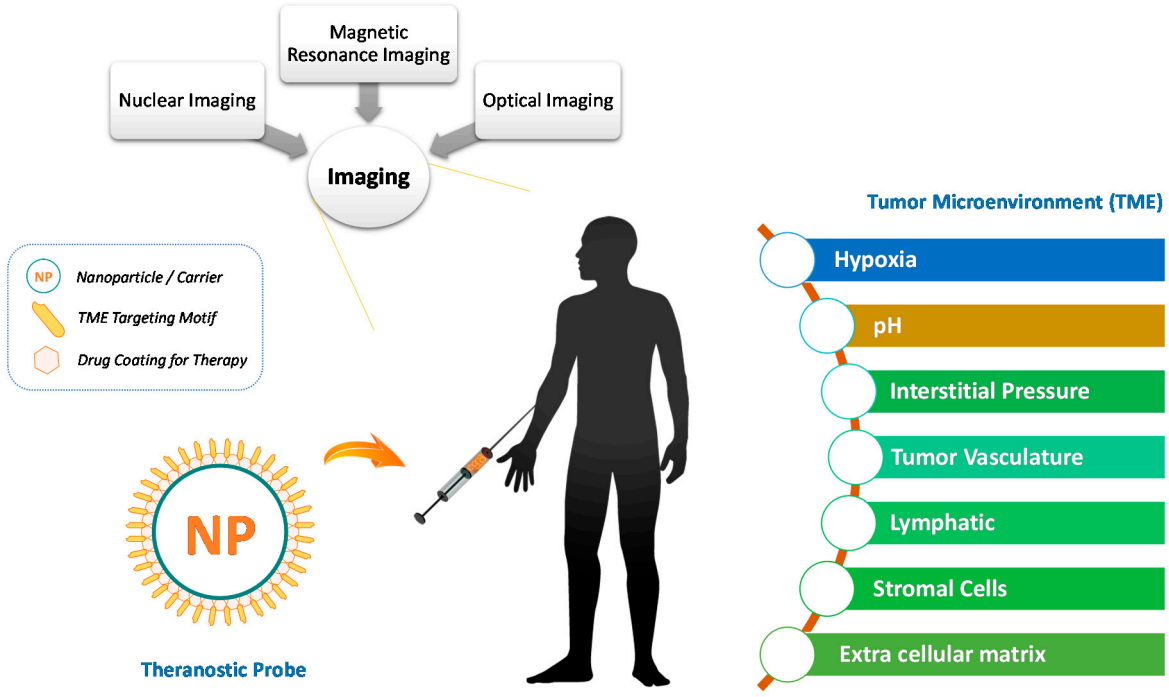

Figure 1. Illustration of theranostic probe incorporated for targeting tumor microenvironment.

2. Tumor Microenvironment Factors

The physical factors which greatly influence the proliferation of the cancer cells are hypoxia, pH and the interstitial pressure in the surrounding environment. These factors also serve as targets for the development of specific theranostic nanoprobes, which will be further discussed in this section.

2.1. Hypoxia

Hypoxia is a state of oxygen deprivation in the tissues. Thomlinson and Gray observed necrotic cells at a diffusion distance around 150 μm off the closest capillaries in human lung cancer cells [13]. They also realized the correlation between hypoxia and the failure of radiation therapy. It was only after the experiments that they discovered the failure was due to the diminished levels of free radicals in the hypoxic cells.

As four decades had passed, it was discovered that the Hypoxia-inducible factors (HIF) consisting HIF-1 and HIF-2, activated gene transcription for the expression of the phenotypes associated with cancer cells [14]. The hypoxic tumor cells can be caused by the limited diffusion of oxygen (chronic) or vasculature collapse (acute) [15,16]. HIF binds to Hypoxia Response Elements (HREs) to maintain the state of oxygen deficiency in cancer cells, so that they can continue carrying out invasion, progression, metastasis and hindrance to radiation therapy [17]. The early attempts to target hypoxia with radiation sensitizers and hyperbaric oxygen failed to be precise, thereby it demands for precise optimization techniques [18]. Thus, the discoveries of therapeutic agents that inhibit HIF-1 are a prominent choice for cancer therapy. Examples of HIF inhibitors are HIF specific single interference RNA and antisense RNA that suppress the invasion and metastasis in pancreatic adenocarcinoma [19].

Several molecular imaging modalities targeting tumor hypoxia such as Positron Emission Tomography (PET), Single Photon Emission computer tomography (SPECT), Magnetic Resonance Imaging (MRI) and optical imaging had been developed. In the upcoming section, nanotheranostic probes targeted on tumor hypoxia and their corresponding imaging modalities will be discussed.

PET imaging of hypoxia for *in vivo* detection is based on the capability of the molecules to bind with the deoxygenated cells using the imaging probes namely, ^{18}F- fluoromisonidazole (^{18}F-FMISO),

Preprints (www.preprints.org) | NOT PEER-REVIEWED | Posted: 13 February 2017 doi:10.20944/preprints201702.0037.v1

^{61}Cu-diacetyl-*bis*(*N*4-methylsemicarbazone) (^{61}Cu-ATSM), 18F-flortanidazole (18F-HX4) etc. The FMISO PET determined the severity of tumors in a case study conducted on 22 patients with glioblastoma multiform (GBM). It was found that the signal intensity of the image correlated with the severity of hypoxia in cancer cells [20,21]. In addition, ^{61}Cu-ATSM PET elevated the contrast for intensity-modulated therapy in head and neck cancer, but this method required precise dosage of radionuclides attached to prodrug or theranostic agents [22]. Despite the advancement of all these probes, PET imaging to target hypoxia in tumors is still confined in the research domain. **Figure 2** shows the results of a dynamic PET scan and evolution of ^{18}F-fluoromisonidazole distribution within patient from initial blood pool to selective sequestration within hypoxic tumor subvolume [23].

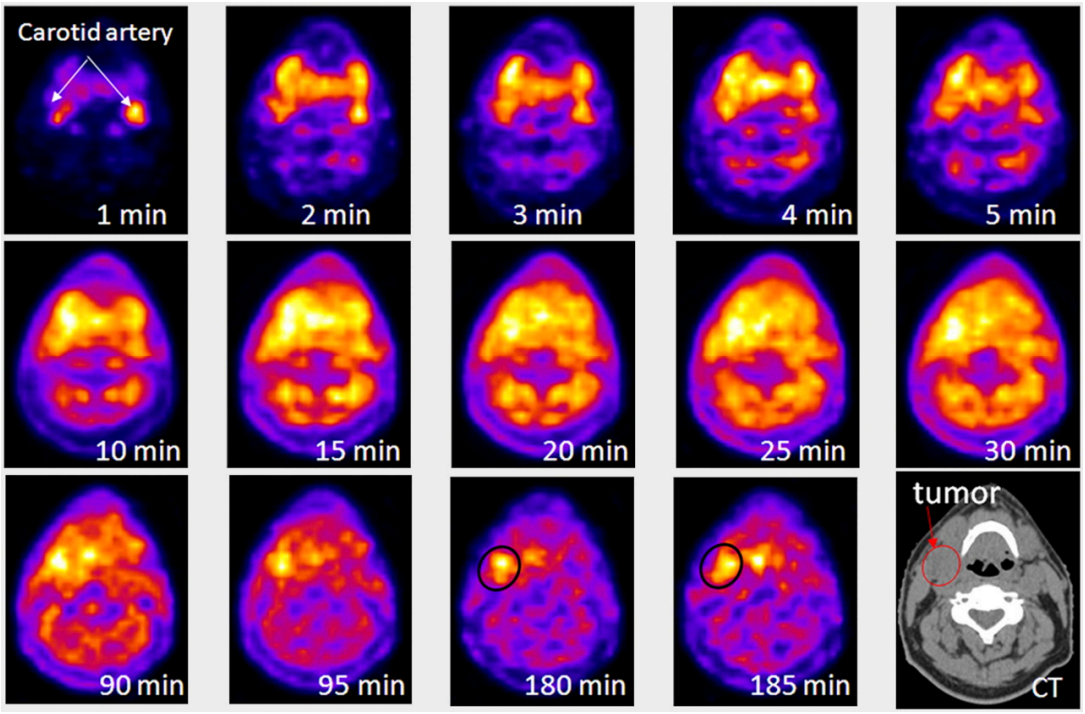

Figure 2: Results of a dynamic PET scan as a function of time after injection with ^{18}F-fluoromisonidazole. Single reconstructed PET slice is displayed through center of head and neck tumor. First 5 frames were of 1-min duration, followed by 5 frames of 5-min duration. At 30 min after injection, patient was removed from scanner and then reimaged at 90 min and 180 min after injection. Images were coregistered using low-dose CT scan (depicted in final image in series). This series shows evolution of ^{18}F-fluoromisonidazole distribution within patient from initial blood pool to selective sequestration within hypoxic tumor subvolume. *This research was originally published in JNM. Carlin, Sean, and John L. Humm. PET of hypoxia: current and future perspectives. J Nucl Med. 2012;53.8:1171-1174. © by the Society of Nuclear Medicine and Molecular Imaging, Inc.* [23]

Magnetic Resonance Spectroscopy (MRS) has evolved with probes for determination of the level of deoxygenation using the relaxation of Hexamethyldisoloxane (HMDSO) such as 1H MRS [24]. It measures the tension of oxygen in prostate cancer cells after intravenous injection [25]. Furthermore, perfluorocarbons (19F MRS) are used in combination with nitroimidazole to design a probe, namely 2-nitro-α-[(2, 2, 2-trifluoroethoxy) methyl]-imidazole-1-ethanol, that undergoes reduction when it binds to the endogenous molecules of hypoxic cells. This enables it to determine the severity of hypoxia *in vivo* [26]. Usually, the nitroimidazole-based probe involves the biomarker SR4554, which was experimented on 26 different patients with predominant gastrointestinal cancer [27]. To conduct surface coil acquisition of tumors using 19F MRS, the tumors must be less than 3 cm in diameter and less than 4 cm in depth. To improve the imaging modality, positive contrast enhancement is achieved using gadolinium-tetraazacyclododecane tetraacetic acid monoamide conjugate of 2-nitro-imidazole (GdDO3NI). Not only can it measure the oxygen deficiency in tumors, it can observe the area with low blood vessel perfusion of a xenograft rat model suffering from prostate cancer [28].

 doi:10.20944/preprints201702.0037.v1

Optical Imaging plays an important role in studying the HRE of carcinomatous cells using fluorescent tags [29] . A trial was executed over the xenograft models to draw the relevance between the vasculature and deprivation of oxygen. It is observed in this experiment that hypoxia affects the transport of macromolecules and its metabolism through the spreading of collagen-1 fiber [30]. However, the fluorescent imaging could not provide a more sensitive metabolic imaging in hypoxic tumors as compared to PET imaging.

On the top of the imaging modalities, the advancement in the synthesis of therapeutic genes namely, Cytosine Deaminase (CD) for HRE activation had been developed. The formation of the cytotoxic 5-fluorouracil (5 FU) from the interaction between nontoxic 5-fluorocytosine (5 FC) and CD can be imaged *in vivo* using 19F MRS. This method can be applied using NPs for the delivery of molecular reagents such as siRNA, cDNA and mRNA in clinical trials [31] .

2.2. pH Level

The balance between the extracellular and intracellular pH is achieved using a group of transporters such as Na+/H+ pumps, carbonic anhydrases (CAs) I-XIII [32]. They can stabilize the concentration levels of hydronium ions evolved by cellular metabolism such as glycolysis. The acidic environment is due to the stringent blood perfusion and increased level of glycolytic activity in the tumor cells [33]. With the prior knowledge of abnormal pH in the TME, various theranostic probes will be enumerated below.

Firstly, MRS can monitor the chemical shift of the mild signals from the inorganic phosphate to characterize the variation of the intracellular pH (pHi) using pH marker such as 3-aminopropylphosphonate. As for characterization of extracellular pH (pHe), 31P MRS was used. Unfortunately, the sensitivity of 31P MRS is low which limits the spatial resolution [34]. Thus, the spatial resolution for pHe could be increased in *in vivo* imaging by replacing the probes with 1H MRS namely (imidazol-1-yl)3-ethyoxycarbonylpropionic acid Later, an improved spatial resolution with enhanced contrast for imaging the pHe was achieved using the another 1H MRSI probe namely, 2-(imidazol-1-yl) succinic acid with increased specificity and sensitivity [35].

Kato and Artemony had worked on novel dual-tracer MRI-based theranostic technique to track the drugs released from nanocarriers using the SPION and gadolinium diethylenetriamine-pentaacetic acid bismethylamide (GdDTPA-BMA) [36]. The utilization of SPION implements a domineering negative enhancement over the positive enhancement due to GdDTPA-BMA, thus allowing pH-based theranostic probes to approach deep layered tissues [37].

Optical probes have been designed to image the acidification in tumors using pH- activated near infrared fluorescent (NIRF) probe with an elevated sensitivity and quicker data acquisition. The probe obtains the absorbance and auto-fluorescence to enhance the sensitivity and spatial resolution for deep layered tissues [38]. One of the probes called DilR 783-S can be activated in the acidic state by the breaking of hydrazine bonds, causing fluorescence effect in MDA-MB-435 xenograft model.

However, the available probes are not used in clinical trials so far. Furthermore, another pH probe like Chemical Exchange Saturation Transfer (CEST) is used to image breast cancer in xenograft model with clinically trialed contrast agents of CT such as iopromide [28]. It can determine the correlation between the amide protons of iopromide and the level of pH. The pH was observed to be in the narrow range of 6.3 to 7.2 irrespective of concentration. The pH level of the tissues could also be estimated through hyperpolarized $H_{13}CO_3$ with prior intravenous injection in the *in vivo* detection [39]. The calculation of pH is done using the Henderson-Hasselbalch equation and it was applied in the lymphoma model of preclinical trial.

Besides the usage of imaging probes to track the fatality of cancer, there is an urgent need for the design of pH-sensitive carriers for a more specific and effective targeting. Thereby, polymeric micelles are well known pH sensitive hydrophobic carriers used to target the tumors with great specificity because they contain ionizable groups [40]. The hydrophobic drugs can be encapsulated in micelles to function in the acidic state of TME. The typical doxorubicin-encapsulated pH

 doi:10.20944/preprints201702.0037.v1

responsive polymeric micelles have been observed to release the maximum of 70% of the target molecule or drug at the pH level of 6.4, while it stops at the pH of 7.4 [41].The ability of this polymeric micelles to detect the antitumor region had been experimented *in vivo*.

2.3. Interstitial fluid pressure (IFP)

Imbalance in the angiogenic factors like vascular endothelial growth factor (VEGF), matrix metalloproteinase (MMP), angiopoietins leads to the production of abnormal vasculature. Sometimes, the hyperpermeability allows exchange of molecules in the tumor vasculature without any maintenance of gradient. This gives rise to an abnormality in IFP [42].

Recently, non-invasive imaging methods like dynamic contrast enhanced magnetic resonance imaging using Gd-DTPA (gadolinium diethylene-triamine penta-acetic acid) are helpful to analyze IFP. This research used xenograft mouse models of many human cancers. They concluded that, the velocity with which fluid flows correlates well with the magnitude of IFP [43].

Nanoprobes designed for targeted therapy towards this abnormal IFP would help to suppress the rapid angiogenic process. A probe designed to target the IFP of a tumor tissue by sterically stabilized lysosomes was filled with Imatinib, a drug to reduce IFP by inhibiting platelet-derived growth factor receptor (PDGF-R) beta. These lipid vehicles are distributed in the tumor. The reduction of tumor was observed under fluorescence imaging [44]. Development of theranostic probes targeting IFP is an ongoing research and hence not many probes have been reported. However, there are many therapeutic drugs such as Imatinib and anakinra (Interleukin antagonist) that decrease the IFP and increase the drug uptake. However, the effect of these drugs has to be studied carefully and hence hybrid imaging like PET/CT takes a unique role. A research on water-perfusable tissue fraction (PTF) with help of ^{15}O-water PET/CT helped to analyze the outcome of imatinib on the IFP in colorectal cancer [45].

3. Efficient drug delivery system

Efficiency of drug delivery system is the key element to improve the present status for both diagnosis and therapy of cancer. Multifunctional upconversion NPs (UCNPs) have been widely used for effective cancer therapy. These NPs are used in nuclear targeting therapy where it delivers the anti-cancer drug into the cancer cell nucleus and also monitors the process using imaging modalities such as MRI, with the help of trans activator transcription (TAT) peptide, which in turn utilized as a cell penetrating peptide (CPP) derived from human immunodeficiency virus 1 (HIV-1) and thus, efficiently helps for the uptake of the NP [46]. The multifunctional UCNP drug delivery system carries the gene with anticancer drug (DOX), which replaces the mutated gene and also, induces the apoptosis of tumor cell by damaging the DNA [47].

3.1. pH based drug delivery system

The graphene-based nanomedicine, also called pH responsive chemotherapy, is used in various type of cancer treatments. Zheng et al. conducted a study to explore the efficiency of graphene NPs in both drug delivery as well as imaging probe. They inferred that these NPs have greater surface area which increases the amount of drug loaded on a single NP [48]. These nanocarriers efficiently deliver the doxorubicin to the cancer nucleus in order to overexpress the HPR2 antibodies which in turn would make high internalization with the cancer nucleus. In the field of pH-based theranostics, Bae et al. prepared the black copolymer NP spherical in shape it carries the anticancer drug. The copolymer form PEG and poly amino acid linkage with hadrazone helps to release the cancer drug in the pH environment [94].

3.2. Enzyme-based nanomedicine

The mesoporus silica nanoparticle (MSN) is another type of efficient drug delivery system that acts as a novel vehicle for the transport of anti-cancer drug, which provides large structural central cavity for drug storage which in turn improves the rate of accumulation of the drug [49]. This silica-based NP is specifically designed for colonic condition because the anti-cancer drug 5-fluoruracil (5FU) is a

 doi:10.20944/preprints201702.0037.v1

water soluble drug activated by colonic enzyme mixture present in the gastrointestinal (GI) track. The folic acid conjugated florescence-based MSN was found to provide effective cellular uptake in tumor induced mice in an experiment conducted by Pan et al. which was examined using flow cytometry and fluorescent microscopy [50]. These MSNs also has 2 to 4 nm size porous channels which are used in transportation of macromolecules such as lipid, protein, and enzyme [51].

3.3. Liposome mediated drug

Liposomal formulated nanostructures are most widely used method for treatment of various types of cancer [52]. The liposome-mediated drug is mostly made up of phospholipid or hydrophilic component to facilitate penetration through the cell membrane. This increases the retention time of drug, when present in higher concentration, and the adhesive nature of tumor tissue. For example, the oral administration of liposome nanocarrier drug binds with negatively charged mucosal membrane present in the intestine and induces the overexpression of receptor which bind to the liposomal nanoprobe.

3.4. Activity based nano theranostics

The enzyme- or protein-based NPs doped with theranostic drugs usually targets the peptides, receptors or any particular small enzymes on the surface of the cell membrane [53]. In the case of cancer-specific enzyme based NPs, the predominantly chosen targets are transferrin receptor protein or glycoproteins which are present in higher quantity in the surface of a cancer cell. These proteins create moieties with the drug-doped NP and enter into the cell through endocytosis [7].

3.5. Nanoparticle based theranostics

There are different types of NP used in the theranostics field especially for cancer treatment. The NPs come in various shapes such as nanodisk, nanorod and worm-like micelle and each of these structures have different drug efficiencies [54]. Amongst these options, spherical-shaped NP is preferred widely especially for targeting TME. It is preferred because of its ability to carry greater volume of drug compared to other shaped-nanoprobe. Non-spherical structures are utilised when the target of the probe is to eliminate the bacteria and evade the immune system attacks [7]. For example, Discher et al. proved the worm-like micelle NP is highly efficient for anticancer drug delivery system which enhances the cellular uptake and improves drug accumulation in the tumor cells [47].

4. Theranostic Probes for Tumor Microenvironment

TME is a key player in the development and progression of cancer. It can be targeted to suppress the severity of cancer. The need for nanoprobes has taken importance in the current research because of the limitations of conventional therapies for cancer treatment. The following section will give an insight on the various therapeutic and imaging probes developed so far to target various components of TME.

4.1. Tumor Vasculature

When a tumor is developing, it needs to be supplied with new blood vessels. The vessel formation (angiogenesis) does not happen sequentially and hence it has increased permeability and leaky membranes. Because of this malformed vasculature, it becomes difficult for drug delivery. Hence, these days nano-therapeutic applications have emerged to tackle the drug delivery inefficiency [42].

A theranostic probe was developed by coating the NPs with photofrin, a photodynamic agent which acts like a sensitizer that is taken up by tumor and undergoes photo irradiation to release singlet oxygen. The photofrin-coated super paramagnetic iron oxide nanoparticle (SPION) was used as an MRI contrast agent. This was further coated with polyethylene glycol (PEG) along with F3 peptide targeted towards tumor vasculature and this was again tagged with a fluorophore Alexa Fluor 594. The *in vitro* and *in vivo* studies showed significant reduction in the tumor size which was visualized *in vivo* using diffused MRI with 2D reconstruction [55]. A probable disadvantage is that photofrin

Preprints (www.preprints.org) | NOT PEER-REVIEWED | Posted: 13 February 2017 doi:10.20944/preprints201702.0037.v1

remains in the skin for a long time, causing patients' skin to be photosensitive for weeks. The tissue penetration for this probe could be difficult due to presence of photofrin.

Schmider et al. developed a probe to target neo-vasculature expressing $\alpha_5\beta_1$ integrin and these vessels were observed with 3D spatial resolution of the MR signals. They did another experiment with a theranostic nanoprobe targeted towards $\alpha_5\beta_1$ ($\alpha_v\beta_3$) integrin along with a fumagillin drug. Results showed a significant reduction in tumor size compared to $\alpha_v\beta_3$ fumigillin which did not show much reduction [56]. The advantage of using 3D reconstructions of the MR signal is that, we can clearly depict the volume of tumor reduction to accurately identify the therapeutic effect of the probe.

Another research conducted by Grange et al. observed that Neural Cell Adhesion Molecule (NCAM) expressed on tumor endothelial cells or Kaposi Cells can be particularly targeted with a specific NCAM peptide. A comparison was made between a PEG liposome with no specific NCAM target and C3d liposome which had a specific peptide moiety. They concluded that C3d liposome was more efficient in delivering the doxorubicin drug into the tumor cell which resulted in a reduction in tumor size and also with less toxicity of the drug. On the other hand, the PEG liposome was accumulated extracellularly. The doxorubicin drug release was observed through MRI by tagging the liposome with a gadolinium– 1,4,7,10-tetraazacyclododecane-1,4,7,10-tetraacetic acid (DOTA) – monoamide or Gd DOTAMA $(C18)_2$ in short [57]. Gd DOTAMA, an important contrast agent, is capable of determining specific signatures of the TME.

Similarly, another study with Gd DOTAMA as a contrast agent in targeting tumor vasculature where a glucocorticoid drug prednisolone phosphate (PLP) was incorporated inside the long circulating stealth liposomes (LCL) and this combination of LCL-PLP could permeate through the tumor vasculature easily compared to normal endothelial cells to achieve a targeted therapeutic effect. Two kinds of drug release study were conducted: one with just LCL-PLP and other with an MRI imaging agent Gd-PLP-LCL. The latter helped to understand the distribution of drug delivered *in vivo* and concluded that this had good accuracy of analyzing the therapeutic response [58].

Advancements such as using magnetic NPs like SPION with a siliceous coating and tagging it with a fluorophore can target the tumor tissue specifically. A Nickel (Ni) micro mesh placed on tumor as well as the SPIONs can get magnetized by an external strong magnet field [59]. With the help of magnetic NPs, size and distance constraints for targeting the required tissue are reduced.

VEGF regulates tumor angiogenesis and is present in excessive amount in a tumor tissue. ^{89}Zr bevacizumab helps to target VEGF-A in breast cancer patients using PET imaging modality. Similarly ^{124}I-VG67e is a monoclonal antibody that binds to VEGF-A that can be imaged through PET [60,61]. To target the VEGF receptor, probes such as ^{64}Cu-DOTA-$VEGF_{121}$ is used where DOTA acts as a chelator [62]. 124-L19-SIP monoclonal antibody was targeted against extra domain- B of fibronectin [63] (as shown in **Figure 3**). ^{123}I-L19$(scFv)_2$ targeted towards fibronectin an imaged by SPECT/CT modality [64]. SPECT imaging modality is also useful for detecting angiogenesis markers with help of probes like 99mTc-scVEGF targeted towards VEGF receptor [65]. VEGF121-Avi-streptavdidn IRDye800scVEGF/Cy is a probe which uses optical imaging or NIRF for detecting VEGF receptor [66].

Preprints (www.preprints.org) | NOT PEER-REVIEWED | Posted: 13 February 2017 doi:10.20944/preprints201702.0037.v1

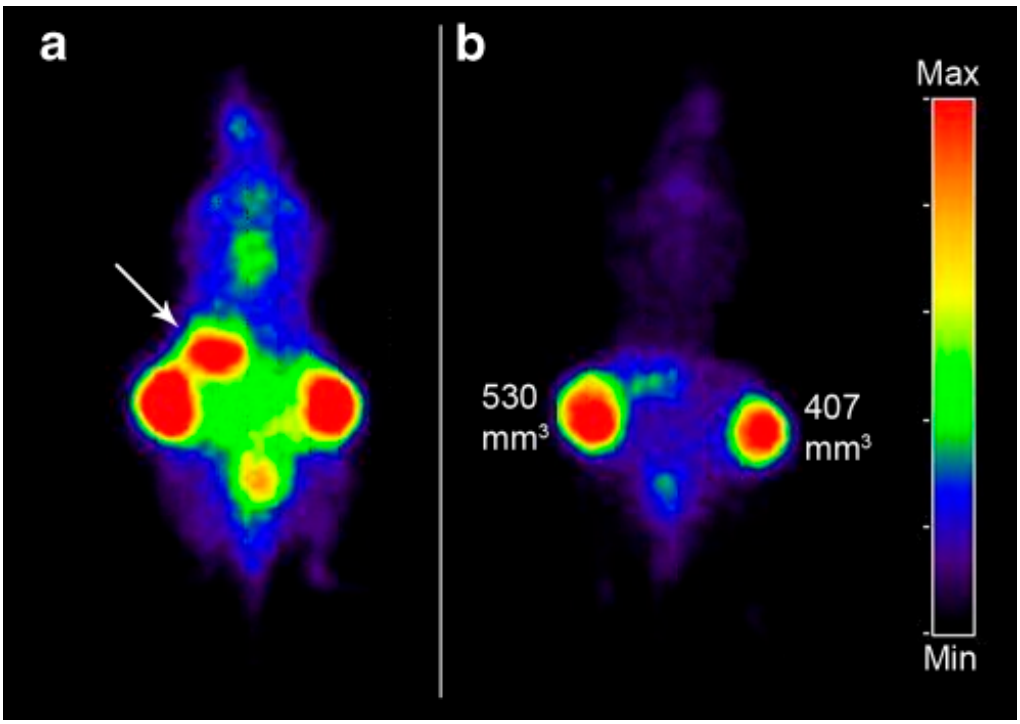

Figure 3. PET images of FaDu xenograft-bearing nude mouse injected with ^{124}I-L19-SIP (3.7 MBq, 25 μg). Coronal images were acquired at 24 (a) and 48 h (b) after injection. Image planes have been chosen where both tumors were visible. Uptake of ^{124}I in the stomach (*arrow*) and to some extend in bladder (urine) is visible at 24 h p.i., but has disappeared at 48 h p.i. *This research was originally published in European Journal of Nuclear Medicine and Molecular Imaging. Bernard M. Tijink. 124I-L19-SIP for immune PET imaging of tumour vasculature and guidance of 131I-L-19SIP radioimmunotherapy © 2016 Springer International Publishing AG* [63].

4.2. Lymphatic System

The lymphatic system is important for both the immune system and spreading cancer to various distant organs, i.e. cancer metastasis. In many diseases including cancer, there is an excess growth of lymphatic vessels (lymphangiogenesis) [67]. Lymphatic endothelial cells express specific antigens such as podoplanin, lymphatic vessel endothelial hyaluronan receptor 1 (LYVE-1) and VEGFR3. The presence of podoplanin on lymphatic endothelial cells promotes their migration, adhesion and lymphatic formation. Yang et al. developed the nanoprobe to target the podoplanin in lymphangiogenesis. They prepared the PEG-GoldMag NPs which were conjugated with anti-podoplanin antibody (PodAb). Later they evaluated the tumor lymphangiogenesis *in vitro* using MRI in breast cancer model [68].

Lymphatics-homing peptide-1 (LyP-1) is a 9-amino-acid cyclic peptide binds to its receptor (p32/gC1qR) in some type of tumor cells especially in highly malignant breast tumor cells MDA-MB-231 and MDA-MB-435S [69]. Luo et al. synthesized an NP specific to tumor lymphatics conjugated with LyP-1 [70]. They used copolymers of maleimide–PEG–poly(lactic-co-glycolic) acid (PLGA) which were conjugated with fluorescein isothiocyanate (FTIC) labelled LyP-1. They found eight times uptake of LyP-1-NPs *in vivo* than only NPs, used for comparing efficacy. The detection of FITC positive cells was done with fluorescence microscopy. In 2011, Zhang et al. also labelled LyP-1 peptide with Cy5.5 (a near-infrared fluorophore) for visualizing under optical imaging [71]. Later in 2012, Wang et al. prepared another NP with LyP-1 conjugated PEG-PCL micelles (LyP-1-PM) and Artemisinin (ART) (a natural anti-cancer and anti-lymphangiogenesis drug). Micelles with artemisinin drug (LyP-1-PM-ART) were observed to have higher antitumor efficacy. LyP-1-PM-ART was found to be very specifically targeting lymphatic tumor tissue as compared to PM-ART which was unnecessarily accumulated in the blood. They used 10-dioctadecyl-3,3,30,30-tetramethylindodicarbocyanine-4-chlorobenzene-sulfonate salt (DiD)-loaded LyP-1-PM or PM with

Preprints (www.preprints.org) | NOT PEER-REVIEWED | Posted: 13 February 2017 doi:10.20944/preprints201702.0037.v1

near-infrared fluorescent imaging in mice as shown in Figure 4 and concluded that the synthesized probe is capable of performing theranostic application for highly metastatic breast tumor and tumor lymphatics [72].

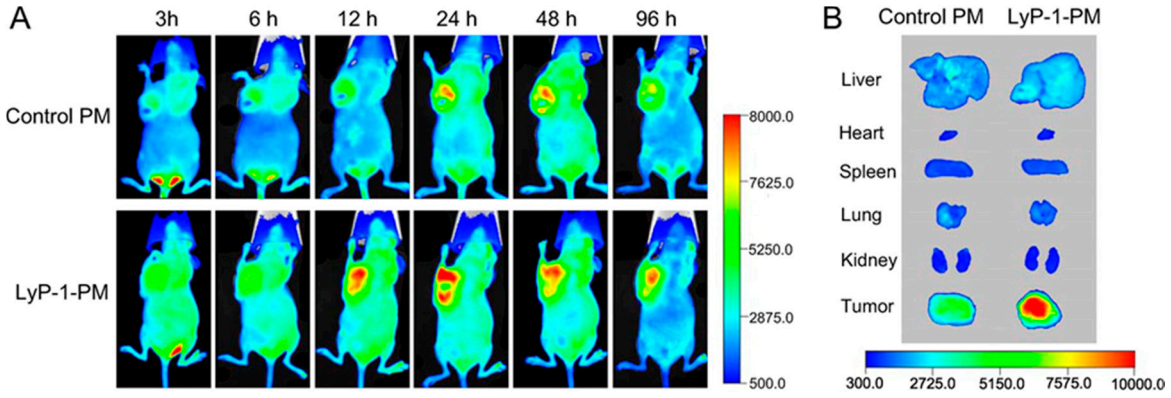

Figure 4: The targeted delivery of LyP-1-PM to highly metastatic breast tumor *in vivo*. (A) *In vivo* near-infrared fluorescent images of mice after intravenous administration of DiD-loaded LyP-1-PM or PM at different time points and (B) *ex vivo* image of tumors and organs after the tumor-bearing mice above were sacrificed at 96 h. *Reprinted with permission from* [72]. *Copyright 2009 American Chemical Society.*

4.3. Extracellular matrix

Changes in rigidity of the ECM can be a trigger for the tumor development. Therefore, when nanocarriers are targeted to this lineage of TME to stop these changes associated with ECM, the growth of tumor can be suppressed.

Hyaluronan (HA) metabolism is a predominant feature for breast cancer progression. During tumor progression, the amount of hyaluronidases is at increased levels. Peer and Margalit discussed about HA tagged to gold NPs along with a fluorophore helps to detect the cancerous tissue due to increased levels of hyaluronidases [73].

Nanotherapeutic probe based on this principle was designed by attaching an antibody of lysyl oxidase to poly (D,L-lactide-co-glycolide)-block-PEG copolymer. This nanoprobe system was successfully implemented *in vitro* and *in vivo* and resulted in significant tumor suppression. The research team conducted a fluorescence spectroscopic analysis using Coumarin-6 dye helped to analyze the nanoprobe accumulation inside the tumor [74].

Proteases that are released by stromal cells help to give property of shape to ECM in tumor cells. These proteases are released excessively and cause the degradation of ECM. Probes targeting the activity of protease will help to image the tumor progression using FRET (Fluorescence Resonance Energy Transfer), NIR imaging.

MMP-2 is usually over expressed in certain tumors. A probe that follows FRET principle was designed by attaching a low molecular weight heparin associated with quantum dot and this moiety was attached to the low molecular weight protamine which contains the MMP-2 substrate cleavable by MMP-2. This substrate acts as a spacer and also contains the fluorophore. MMP-2 overexpressed in the tumor tissue will cleave this spacer leaving the fluorophore free. To make this probe permeable through the blood brain barrier (BBB), a transferrin receptor T7 peptide was used for targeting the tumor correctly [75].

A recent advancement in this field is the usage of external alternate magnetic field which makes the liposomes covered by heat sensitive magnetic NPs to undergo hysteresis and this localized increase in temperature triggers the release of protease substrates embedded inside the liposome. MMPs

Preprints (www.preprints.org) | NOT PEER-REVIEWED | Posted: 13 February 2017 doi:10.20944/preprints201702.0037.v1

excessively present on tumor tissues will degrade the substrate and these short peptides will be detected by diagnostic tests like enzyme-linked immunosorbent assay (ELISA) [76].

Collagen undergoes many changes in the TME. These structural proteins get denatured due to action by MMPs and several other proteases. Collagen mimetic peptides are photo-triggered and have a tendency to form a triple helix with the denatured collagen. The CMPs were tagged with Near Infrared Fluorophore (NIRF) (IR-Ahx-$(GPO)_9$) and fluorescence revealed the accumulation of the triple helical structure in the tumor tissue [77].

4.4. Stromal cells

Tumor- associated stromal cells (TASCs) such as cancer- associated fibroblasts (CAFs) and tumor-associated macrophages (TAMs) had been found to play a key role in promoting cancer progression and metastasis [78–80]. CAFs are widely seen in breast and pancreatic cancer [81,82]. The overexpression of fibroblast activation protein-α (FAP) (membrane bound serine protease), on the CAFs, makes them different from the normal stromal cells [83]. FAP has a unique post-prolyl endopeptidase activity to cleave the dipeptide at NH_2-terminal [84,85]. Hence, FAP-α is known to give shape to microenvironment which promotes growth as well as invasion of tumor through degrading ECM [86–88]. Ji et al. designed the ferritin-based FAP-α responsive fluorescence probe for the imaging of CAF-positive cancers. Since FAP-α is excessively present in tumor tissue, the ferritin-based fluorescence-tagged peptide on the probe will get cleaved by the FAP-α to release the fluorophore and get detected. *In vivo* imaging also had been done by Ji and colleagues in mice when these nanoprobes were injected intravenously [89]. Ji et al. also designed a novel nanocarrier made up of a cleavable amphiphilic peptide (CAP), encapsulated with hydrophobic drug doxorubicin (Dox) to target CAFs in TME. This CAP-Dox-NPs showed excellent results in terms of both specificity and antitumor activity when examined under *in vivo* fluorescence imaging [90].

Furthermore, cysteine cathepsins especially cathepsin B (CtsB) are excessively expressed in TME. Normally, CtsB interacts with lysosomes to perform functions such as autophagy and immune responses [91]. The excess secretion of CtsB by different types of cells present in TME including tumor cells, tumor-associated macrophages (TAM) and fibroblasts, makes them potent cancer-specific target [92]. Mikhaylov et al. developed the liposomal nanocarrier (LNC) that contains CtsB inhibitor (NS-629) to target CtsB in the TME. NS-629 is linked to a PEG-functionalized lipid by a lipid linker to form LNC that can able to target CtsB on tumor (LNC-NS-629). They functionalized LNC-NS-629 by tagging the Gadolinium (Gd) to enhance the contrast at tumor sites when viewed under MRI. After MRI, they found that there was no undesirable accumulation of LNC-NS-629 in normal healthy tissues. Thus, Gd conjugated LNC-NS-629, can be used as a potential diagnostic tool. They also loaded LNC-NS-629 with Alexa Fluor 555 to confirm the target at tissue level when viewed under fluorescence microscopy. Upon examination, only TME cells showed fluorescent LNC-NS-629. Finally, when they encapsulated anticancer drug doxorubicin in LNC-NS-629 to target primary MMTV- PyMT tumor cells, they found that it gives 22-fold more killing result when compared with doxorubicin encapsulated in the LNC liposomes without NS-629 [93].

As mentioned before the role of TAMs in tumor progression, invasion and metastasis, they can also be the potent drug target. The over-expression of mannose receptor on the TAMs was used for targeting the TAMs positive carcinomas [94]. Zhu et al. developed the PEG-sheddable PLGA NP conjugated with mannose as the ligand. PEG shedding is used to lessen the uptake of NPs by normal cells. They quantified the uptake amount (*in vitro* and *in vivo* fate) by labelling PLGA with FITC when viewed under a fluorescence microscope. This system may use to target drugs like Yondelis and bisphosphonate clodronate to TAMs [80]. Nowadays, various agents for Macrophage-specific PET imaging had been designed [95]. M1 and M2 macrophages under TAMs have opposites function, where M1 shows the antitumor activity and M2 is known to show pro-tumorigenic properties. Henceforth, the recent focus shifts to the development of NP which can inhibit the M2 macrophages functions and to convert them into M1 macrophages [96].Table 1 enlists significant probes being incorporated for therapy and imaging of tumor microenvironment.

Preprints (www.preprints.org) | NOT PEER-REVIEWED | Posted: 13 February 2017 doi:10.20944/preprints201702.0037.v1

Table 1: Significant probes being incorporated for therapy and imaging of tumor microenvironment

S No.	Tumor Microenvironment	Imaging Modality	Probe Design	*In Vivo* Model	References
1	Tumor Vasculature	MRI	Photofrin iron oxide coated nanoparticles	Rat glioma	Reddy et al. [55]
2	Tumor Vasculature	MRI	α5β1 RGD (Radiolabeled Arg Gly Asp) rhodamine nano particles	A5β1 integrin in MDA-MD 435 xenograft mouse model	Schmieder et al. [56]
3	Tumor Vasculature	MRI	α5β1(αvβ3) fumagillin	A5β1(αvβ3) in MDA MD 435 xenograft mouse model	Schmieder et al. [56]
4	Tumor Vasculature	MRI	NCAM targeted liposomes with doxorubicin and Gd	SCID male mice	Grange et al. [57]
5	Tumor Vasculature	MRI	PLP-LCL	B16.F10 melanoma cells injected to Male C57BI6 mice	Cittadino et al. [58]
6	Tumor Vasculature	MRI	SPIO magnetic nano particles	EGFP transfected U87MG human glioblastoma into SCID mouse	Fu Aihua et al. [59]
7	VEGF-A	PET	^{89}Zr bevacizumab	Human adenocarcinoma patients	Gaykema et al. [60]
8	VEGF-A	PET	^{124}I-VG67e	HT1080-26.6-bearing mice	Collingridge et al. [97]
9	VEGF Receptor	PET	^{64}Cu-DOTA-VEGF$_{121}$	Mice bearing U87MG human glioblastomas	Ferrara 2009 [62]
10	ED-B of fibronectin	PET	124-L19-SIP	Xenograft nude mice	Tijink et al [63]
11	Fibronectin	SPECT/CT	^{123}I-L19(scFv)$_2$	5 male patients with head and neck cancer	Birchler et al. [64]
12	VEGF Receptor	SPECT	99mTc-scVEGF	Male Swiss–Webster mice	Levashova et al. [65]
13	VEGF Receptor	Near Infrared Fluorescence	VEGF121-Avi-streptavdidn IRDye800scVEGF/Cy	Mice bearing VEGFR-2– expressing 67NR murine breast tumors	Kang et al. 2013 [98]
14	Extracellular Matrix	Optical	HA-Au	C57BL/6 male mice were given a	Peer and

 doi:10.20944/preprints201702.0037.v1

			nanoparticles-Fluorophore	bolus injection of saline or of MMC formulations	Margalit [73]
15	Extracellular Matrix	Optical	LOX antibody-copolymer	Mice bearing 4T1 tumors implanted within the mammary fat pad	Kanapathipillai et al. [74]
16	MMP-2	FRET	T7 peptide-LMWH-QD-LMWP-Fluorophore	Xenograft, *ex vivo* and *in vivo* of mice bearing HT1080 tumor	Y. Wang et al. [75]
17	Collagen	Optical	CMP-IR-Ahx-(GPO)9	Prostate cancer cells were implanted subcutaneously in non-obese diabetic (NOD)/ severe-combined immunodeficient (SCID) mice.	Li et al. [77]
18	Hypoxia (deoxygenated cells)	PET	18F-FMISO	Glioblastoma patients	Spence et al. [21]
19	Hypoxia (deoxygenated cells)	PET	61Cu-ATSM	Head and neck squamous cell carcinoma	Flynn et al. [22]
20	Hypoxia (deoxygenated cells)	Magnetic Resonance Spectroscopy (MRS)	1H-MRS	A Meth-A tumor bearing BALB/C mouse was injected with Oxypherol-ET	Flynn et al. Kodibagkar et al. [24] [25]
21	Hypoxia (deoxygenated cells)	MRS	19F MRS	Gastrointestinal cancer	Procissi et al [26]
22	Hypoxia (deoxygenated cells)	MRS	GdDO3NI	Rat prostate cancer	Badalà, Nouri-mahdavi, and Raoof [99]
23	Hypoxia (deoxygenated cells)	Optical Imaging	azo based fluorescent probe	Xenograft models	Kakkad et al. [30]
24	pH	MRS	(imidazol-1-yl) 3-ethyoxycarbonylpropionic acid	Human breast cancer cells (MCF-7 and mdamb-435), grown in the mammary fat pad of severe combined immunodeficient (SCID) mice.	Van Sluis et al. [100]
25	pH	MRS	2-(imidazol-1-	Gliomas in rat brain	Provent et

Preprints (www.preprints.org) | NOT PEER-REVIEWED | Posted: 13 February 2017 doi:10.20944/preprints201702.0037.v1

			yl) succinic acid		al. [35]
26	pH	Optical	DilR-783-S	MDA-MB-435 xenograft model	L. Wang et al. [38]
27	pH	Optical	CEST with iopromide contrast agent	Breast cancer xenograft	Smith et al [28]
28	pH	Optical	doxorubicin - polymeric micelles	B16F10 tumor-bearing mice	Ko et al [41]
29	Stromal Cells (FAP-α)	Optical	ferritin-fluorescence peptide	Co-implants Mice bearing CAFs and PC-3 co implants	Ji et al [89] [90]
30	Stromal Cells (FAP-α)	Optical	CAP-doxorubicin-Nanoparticles	Mice bearing CAFs and PC-3 co implants	Ji et al [89][90]
31	CtsB-PyMT tumor cells	Fluorescence Microscopy	Doxorubicin-LNC-NS629-Gd -Alexa Fluor 555	Mice bearing orthotopically transplanted congenic mammary tumors	Mikhaylov et al [93]
32	CtsB-PyMT tumor cells	Fluorescence Microscopy	mannose-PLGA -FITC	C57BL/6 mice	Zhu et al. [80]
33	Podoplanin	MRI	PEG-GoldMag -nanoparticles-PodAb	Rat breast tumor model	Yang et al. [68]
34	Stromal Cells	Fluorescence microscopy	LyP-1-maleimide-PEG-PLGA -FTIC	Lymphatic metastasis tumor models, Nude BALB/c nu/nu mice	Luo et al. [70]
35	Stromal Cells	Fluorescence microscopy	LyP-1-Cy5.5	4T1 murine breast cancer in mouse	Zhang et al. [71]
36	Stromal Cells	NIR Fluorescent imaging	LyP-1-PM-ART	Nude mice bearing orthotopic MDA-MB-435S breast tumors	Z. Wang et al. [72]
37	Interstitial Fluid Pressure	MRI	Gd-DTPA	Xenograft mouse models	Hompland et al. [43]

5. Challenges in effective cancer theranostics

Nanotechnology is one of the most commonly used techniques for both medical imaging and therapy of cancer theranostics. However, the NPs-assisted imaging faces an obstacle caused by the poor scattering property of the particles [101]. Thus, there is a demand for an increase in the

 doi:10.20944/preprints201702.0037.v1

scattering property of the probes to improve the contrast of the medical image and to develop a more efficient drug delivery.

One of the major challenges faced in nanotheranostics is the stability of the functionalization between the nanoprobe and the particular drug. Though this challenge can be overcome by modifying the surface of the nanoprobe, it gives rise to another problem – the control over the size of the nanostructure. This is because some applications like probes for the brain or liver require a much smaller nanocarrier in order to efficiently penetrate the cells [102]. The efficiency of multifunctional nanocarriers is challenged by the specificity of cancer cell response as different types of cancer cells are responsive to different types of drugs. Similarly, some type of cancer cells can be resistant to particular drugs too. Thus, the position of multifunctional theranostic nanoprobe is not an easy feat in cancer theranostics [103]. However, to overcome the challenge of non-responsive sell receptor, the target may not be the cell itself. The NPs can be made sensitive to external factors of the TME such as pH or temperature [104]. If it is a pH-sensitive NP, it is preferred to be developed as an acidity-activated particle in cancer theranostics as the pH in the TME is usually low, indicating an acidic environment.

Nanotoxicity is an important factor in appraising the safety of the probe's use in future. It also proves to be a major concern in the therapeutic techniques because when the negative interaction between NP and the drug might induce free radical production. This may in turn target the healthy neighbouring cells instead of the cancer cells [105]. This phenomenon defeats the purpose of improving the patients' health by killing the healthy cells. Some nanoprobes may remain in the body even after complete phagocytosis of cancer cells which also leads to nanotoxicity by which the patient may experience side effects. Silicon-based nanoprobes are developed to overcome this obstacle but it is still under research as its speed of delivery appears inadequate [53]. However, the NPs designed particularly for neuroimaging go through another challenge, which is the need for it to cross the selectively permeable BBB layer. There are not many probes which can overcome this problem. Thus, a lot of research experiments are being conducted in order to find out the transporter that can facilitate the crossing of the BBB layer [103].

In the recent years, attaching immunosuppressors with the nanoprobes seems to be highly welcomed as it eliminates the risk of triggering the immune system thus, possibly leading to autophagy [51]. Autophagy is a phenomenon where the immune cells, triggered by a foreign substance invasion attacks the healthy cells along with the foreign substance which in turn disturbs the metabolic homeostasis [106].

The radioactive imaging probes have an attribute called half-life, which denotes the amount of time it remains active. Usually, the probes have low half-time denoting their poor-viability and thus it demands a faster imaging process [106]. Multifunctional nanocarriers such as liposome and micelles are mostly used for imaging and drug delivery as they have the ability to reduce the side effects, lower the toxicity and increase the uptake of the drug by tumor cells efficiently. However, when compared to metal NPs such as gold or iron oxide NPs, the multifunctional NPs give lesser contrast imaging due to its lipid-like surface [107]. Although gene-based therapy is widely used to treat cancer, it is still not the ultimate treatment due to the lack of knowledge in both prognosis and mechanism of the cancer and TME [52].

6. Conclusion

It is a milestone in cancer research to observe the paradigm shift of cancer cells from an isolated mass of cells displaying uncontrolled division to one that undergoes complicated communication with the TME. Since then, many studies have expanded our knowledge on different components of TME and their roles in tumor development. The rapid advancements in nanotechnology allow nanotheranostics to be implemented in the combat against cancer.

The abnormal pH, interstitial fluid pressure (IFP) and oxygen concentration in the TME serve as suitable target for nanoprobe for cancer detection. Moreover, the difference in the environment of

 doi:10.20944/preprints201702.0037.v1

healthy cells and TME allows researchers to design drug carriers that release anticancer drugs in the TME. However, many of these drug carriers and molecular probes are still confined in the research domain and have yet to be translated in the clinical setting. This review has discussed the methods with which different elements in TME are targeted using nanotheranostics for detection, therapy and drug design in cancer, for example, the tumor-associated stromal cells (TASCs) that consist of tumor-associated macrophages and cancer-associated fibroblast. The overexpression of genes in TASCs poses as a potential nanotheranostic target. Abnormally high level of lymphangiogenesis with overexpression of antigens is also another target for nanotheranostics. Apart from that, scientists had developed different nanoprobes to detect angiogenesis and the proteins attached to the newly made blood vessels using modalities like PET and MR imaging. Besides that, the signaling molecules and growth factors supplied by the ECM for tumor progression have provided potent cancer-specific target nanoprobe development. Lastly, we have highlighted different drug delivery systems designed based on pH, enzyme, liposome and topology. The shortcomings of these drug delivery systems, such as cytotoxicity and instability of functionalization between the drug and the NPs have been discussed.

In conclusion, the rapid knowledge advancement in tumor microenvironment and its role in tumor development proffer researchers a better foundation to conduct cancer research. The development of TME-specific nanotheranostics will provide a faster and more accurate cancer diagnosis and therapy in the future, if it is translated in the clinical setting.

7. Future perspectives

This review highlights the significance of TME in cancer progression. However, the complex and dynamic interactions between different elements in TME and tumors are still not elucidated. Instead of merely studying how one element interacts with tumor cells, more studies should be conducted on the interplay of different components of the TME on tumor cells. Even with the advent of nanotheranostics, many nanoprobes are yet to be implemented in the clinical setting due to the complexity and problems in image acquisition using nanoprobes. This is comprehensible because the diverse interactions of the tumor microenvironment and cancer cells are poorly characterized. Currently, many correlations between elements in the tumor microenvironment and tumors have been established. However, the molecular interactions of the tumor microenvironment and signaling pathways for tumor progression await clearer delineation. By mapping the interactions and pathways, scientist can then have a better understanding of the behaviors of tumor cells. When such comprehension is established, we can then apply nanotheranostics for cancer therapy, targeting and detection.

Acknowledgments: Parasuraman Padmanabhan and Balázs Gulyás acknowledges The Lee Kong Chian School of Medicine, Nanyang Technological University MOE Start-Up Grant and MOE Tier-1 grants (2014-T1-001-229 -1T1 -04/14 and L0421160 -1T1-06/15), Singapore.

Author Contributions: Musafar Gani Sikkandhar, Anu Maashaa Nedumaran, Roopa Ravichandar, Satnam Singh, Induja Santhakumar and Zheng Cong Goh contributed in literature collection and preparation of manuscript. Musafar Gani and Anu Maashaa Nedumaran contributed in designing the layout and compiling the content. Roopa Ravichandar contributed in preparing and incorporating the figures and table. Satnam Singh contributed in editing and formatting the manuscript. Satnam Singh, Anu Maashaa Nedumaran and Zheng Cong Goh contributed in revising the manuscript. Sachin Mishra, Govindaraju Archunan, Balázs Gulyás and Parasuraman Padmanabhan contributed in reviewing, revising and guiding in preparation of manuscript title, layout and content. All authors read and approved the final manuscript.

Conflicts of Interest: The authors declare no conflict of interest.

References

1. Korneev, K. V.; Atretkhany, K.-S. N.; Drutskaya, M. S.; Grivennikov, S. I.; Kuprash, D. V.; Nedospasov, S. A. TLR-signaling and proinflammatory cytokines as drivers of tumorigenesis. *Cytokine* **2017**, *89*, 127–135.

2. Spill, F.; Reynolds, D. S.; Kamm, R. D.; Zaman, M. H. Impact of the physical microenvironment on tumor progression and metastasis. *Curr. Opin. Biotechnol.* **2016**, *40*.

3. Wu, Y.; Zhang, W.; Li, J.; Zhang, Y. Optical imaging of tumor microenvironment. *Am. J. Nucl. Med. Mol. Imaging* **2013**, *3*, 1–15.

4. Thiruppathi, R.; Mishra, S.; Ganapathy, M.; Padmanabhan, P.; Gulyás, B. Nanoparticle Functionalization and Its Potentials for Molecular Imaging. *Adv. Sci.* **2016**.

5. Haigron, P.; Dillenseger, J.-L.; Limin Luo; Coatrieux, J.-L. Image-Guided Therapy: Evolution and Breakthrough. *IEEE Eng. Med. Biol. Mag.* **2010**, *29*, 100–104.

6. Chi, C.; Du, Y.; Ye, J.; Kou, D.; Qiu, J.; Wang, J.; Tian, J.; Chen, X. Intraoperative Imaging-Guided Cancer Surgery: From Current Fluorescence Molecular Imaging Methods to Future Multi-Modality Imaging Technology. *Theranostics* **2014**, *4*, 1072–1084.

7. Jo, S. D.; Ku, S. H.; Won, Y.-Y.; Kim, S. H.; Kwon, I. C. Targeted Nanotheranostics for Future Personalized Medicine: Recent Progress in Cancer Therapy. *Theranostics* **2016**, *6*, 1362–1377.

8. Kim, J. B.; Park, K.; Ryu, J.; Lee, J. J.; Lee, M. W.; Cho, H. S.; Nam, H. S.; Park, O. K.; Song, J. W.; Kim, T. S.; Oh, D. J.; Gweon, D.; Oh, W.-Y.; Yoo, H.; Kim, J. W. Intravascular optical imaging of high-risk plaques *in vivo* by targeting macrophage mannose receptors. *Sci. Rep.* **2016**, *6*, 22608.

9. Hatzimanolis, A.; McGrath, J. A.; Wang, R.; Li, T.; Wong, P. C.; Nestadt, G.; Wolyniec, P. S.; Valle, D.; Pulver, A. E.; Avramopoulos, D. Multiple variants aggregate in the neuregulin signaling pathway in a subset of schizophrenia patients. *Transl. Psychiatry* **2013**, *3*, e264.

10. Padmanabhan, P.; Kumar, A.; Kumar, S.; Chaudhary, R. K.; Gulyás, B. Nanoparticles in practice for molecular-imaging applications: An overview. *Acta Biomater.* **2016**, *41*, 1–16.

11. Sridhar, S.; Mishra, S.; Gulyás, M.; Padmanabhan, P.; Gulyás, B. An Overview of Multimodal Neuroimaging Using Nanoprobes. *Int. J. Mol. Sci.* **2017**, *18*, 311.

12. Yu, M. K.; Park, J.; Jon, S. Targeting Strategies for Multifunctional Nanoparticles in Cancer

Imaging and Therapy. *Theranostics* **2012**, *2*, 3–44.

13. Thomlinson, R. H.; Gray, L. H. The Histological Structure of Some Human Lung Cancers and the Possible Implications for Radiotherapy. *Br. J. Cancer* **1955**, *9*, 539–549.

14. Chen, Y.-Q.; Zhao, C.-L.; Li, W. Effect of hypoxia-inducible factor-1alpha on transcription of survivin in non-small cell lung cancer. *J. Exp. Clin. Cancer Res.* **2009**, *28*, 29.

15. Bussink, J.; Kaanders, J. H. A. M.; Rijken, P. F. J. W.; Raleigh, J. A.; Kogel, A. J. Van Der Changes in Blood Perfusion and Hypoxia after Irradiation of a Human Squamous Cell Carcinoma Xenograft Tumor Line. **2000**, *404*, 398–404.

16. Manuscript, A.; Brown, A.; Brown, S.; Ellisor, D.; Hagan, N.; Zervas, M. NIH Public Access. *Cell* **2010**, *29*, 1–7.

17. Erler, J. T.; Bennewith, K. L.; Nicolau, M.; Dornhöfer, N.; Kong, C.; Le, Q.-T.; Chi, J.-T. A.; Jeffrey, S. S.; Giaccia, A. J. Lysyl oxidase is essential for hypoxia-induced metastasis. *Nature* **2006**, *440*, 1222–6.

18. Michieli, P. Hypoxia, angiogenesis and cancer therapy: To breathe or not to breathe? *Cell Cycle* **2009**, *8*, 3291–3296.

19. Semenza, G. HIF-1 Inhibitors for Cancer Therapy: From Gene Expression to Drug Discovery. *Curr. Pharm. Des.* **2009**, *15*, 3839–3843.

20. Penet, M.-F.; Krishnamachary, B.; Chen, Z.; Jin, J.; Bhujwalla, Z. M. Molecular Imaging of the Tumor Microenvironment for Precision Medicine and Theranostics. In *Advances in cancer research*; 2014; Vol. 124, pp. 235–256.

21. Spence, A. M.; Muzi, M.; Swanson, K. R.; Sullivan, F. O.; Jason, K.; Rajendran, J. G.; Adamsen, T. C. H.; Link, J. M.; Swanson, P. E.; Yagle, K. J.; Rostomily, R. C.; Silbergeld, D. L.; Krohn, K. A. Radiotherapy◎: Correlation with Time to Progression and Survival. **2015**, *14*, 2623–2630.

22. Flynn, R. T.; Bowen, S. R.; Bentzen, S. M.; Mackie, T. R.; Jeraj, R. Intensity modulated x-ray (IMXT) vs. proton (IMPT) therapy for theragnostic hypoxia-based dose painting. *Phys Med Biol.* **2008**, *53*, 4153–4167.

23. Carlin, S.; Humm, J. L. PET of hypoxia: current and future perspectives. *J. Nucl. Med.* **2012**, *53*, 1171–1174.

24. Mason, R. P.; Shukla, H.; Antich, P. P. *In vivo* oxygen tension and temperature: Simultaneous determination using19F NMR spectroscopy of perfluorocarbon. *Magn. Reson. Med.* **1993**, *29*, 296–302.

25. Kodibagkar, V. D.; Cui, W.; Merritt, M. E.; Mason, R. P. Novel 1H NMR approach to quantitative tissue oximetry using hexamethyldisiloxane. *Magn. Reson. Med.* **2006**, *55*, 743–748.

26. Procissi, D.; Claus, F.; Burgman, P.; Koziorowski, J.; Chapman, J. D.; Thakur, S. B.; Matei, C.; Ling, C. C.; Koutcher, J. A. *In vivo* 19F magnetic resonance spectroscopy and chemical shift imaging of tri-fluoro-nitroimidazole as a potential hypoxia reporter in solid tumors. *Clin. Cancer Res.* **2007**, *13*, 3738–3747.

27. Lee, C. P.; Payne, G. S.; Oregioni, a; Ruddle, R.; Tan, S.; Raynaud, F. I.; Eaton, D.; Campbell, M. J.; Cross, K.; Halbert, G.; Tracy, M.; McNamara, J.; Seddon, B.; Leach, M. O.; Workman, P.; Judson, I.

A phase I study of the nitroimidazole hypoxia marker SR4554 using 19F magnetic resonance spectroscopy. *Br. J. Cancer* **2009**, *101*, 1860–1868.

28. Smith, J.; Morgan, J. R.; Zottoli, S. J.; Smith, P. J.; Buxbaum, J. D.; Bloom, O. E. Regeneration in the era of functional genomics and gene network analysis. *Biol. Bull.* **2011**, *221*, 18–34.

29. Raman, V.; Artemov, D.; Pathak, A. P.; Winnard, P. T.; McNutt, S.; Yudina, A.; Bogdanov, A.; Bhujwalla, Z. M. Characterizing vascular parameters in hypoxic regions: A combined magnetic resonance and optical imaging study of a human prostate cancer model. *Cancer Res.* **2006**, *66*, 9929–9936.

30. Kakkad, S. M.; Solaiyappan, M.; Argani, P.; Sukumar, S.; Jacobs, L. K.; Leibfritz, D.; Bhujwalla, Z. M.; Glunde, K. Collagen I fiber density increases in lymph node positive breast cancers: pilot study. *J. Biomed. Opt.* **2012**, *17*, 116017.

31. Konishi, M.; Kawamoto, K.; Izumikawa, M.; Kuriyama, H.; Yamashita, T. Gene transfer into guinea pig cochlea using adeno-associated virus vectors. *J. Gene Med.* **2008**, *10*, 610–618.

32. Stock, C.; Schwab, A. Protons make tumor cells move like clockwork. *Pflugers Arch. Eur. J. Physiol.* **2009**, *458*, 981–992.

33. Gillies, R. J.; Robey, I.; Gatenby, R. A. Causes and consequences of increased glucose metabolism of cancers. *J Nucl Med* **2008**, *49 Suppl 2*, 24S–42S.

34. Robey, I. F.; Baggett, B. K.; Kirkpatrick, N. D.; Roe, D. J.; Sloane, B. F.; Hashim, A. I.; Morse, D. L.; Gatenby, R. a; Gillies, R. J. NIH Public Access. **2010**, *69*, 2260–2268.

35. Provent, P.; Benito, M.; Hiba, B.; Farion, R.; López-Larrubia, P.; Ballesteros, P.; Rémy, C.; Segebarth, C.; Cerdán, S.; Coles, J. A.; García-Martín, M. L. Serial *in vivo* spectroscopic nuclear magnetic resonance imaging of lactate and extracellular pH in rat gliomas shows redistribution of protons away from sites of glycolysis. *Cancer Res.* **2007**, *67*, 7638–7645.

36. Kalash, R.; Berhane, H.; Au, J.; Rhieu, B. H.; Epperly, M. W.; Goff, J.; Dixon, T.; Wang, H.; Zhang, X.; Franicola, D.; Shinde, A.; Greenberger, J. S. Differences in irradiated lung gene transcription between fibrosis-prone C57BL/6NHsd and fibrosis-resistant C3H/HeNHsd mice. *In Vivo* **2014**, *28*, 147–171.

37. Moon, S.-H.; Yang, B. Y.; Kim, Y. J.; Hong, M. K.; Lee, Y.-S.; Lee, D. S.; Chung, J.-K.; Jeong, J. M. Development of a complementary PET/MR dual-modal imaging probe for targeting prostate-specific membrane antigen (PSMA). *Nanomedicine Nanotechnology, Biol. Med.* **2016**, *12*, 871–879.

38. Wang, L.; Zhu, X.; Xie, C.; Ding, N.; Weng, X.; Lu, W.; Wei, X.; Li, C. Imaging acidosis in tumors using a pH-activated near-infrared fluorescence probe. *Chem. Commun.* **2012**, 1–23.

39. Gallagher, F. A.; Kettunen, M. I.; Day, S. E.; Hu, D.-E.; Ardenkjær-Larsen, J. H.; Zandt, R. in 't 't R. in /`t; Jensen, P. R.; Karlsson, M.; Golman, K.; Lerche, M. H.; Brindle, K. M.; Ardenkjaer-Larsen, J. H.; Zandt, R. in 't 't R. in /`t; Jensen, P. R.; Karlsson, M.; Golman, K.; Lerche, M. H.; Brindle, K. M.; Ardenkjær-Larsen, J. H.; Zandt, R. in 't 't R. in /`t; Jensen, P. R.; Karlsson, M.; Golman, K.; Lerche, M. H.; Brindle, K. M. Magnetic resonance imaging of pH *in vivo* using hyperpolarized 13C-labelled bicarbonate. *Nature* **2008**, *453*, 940–943.

40. Gao, G. H.; Li, Y.; Lee, D. S. Environmental pH-sensitive polymeric micelles for cancer diagnosis and targeted therapy. *J. Control. Release* **2013**, *169*, 180–184.

41. Ko, J.; Park, K.; Kim, Y. S.; Kim, M. S.; Han, J. K.; Kim, K.; Park, R. W.; Kim, I. S.; Song, H. K.; Lee, D. S.; Kwon, I. C. Tumoral acidic extracellular pH targeting of pH-responsive MPEG-poly(β-amino ester) block copolymer micelles for cancer therapy. *J. Control. Release* **2007**, *123*, 109–115.

42. Siegler, E. L.; Kim, Y. J.; Wang, P. Nanomedicine targeting the tumor microenvironment: therapeutic strategies to inhibit angiogenesis, remodel matrix, and modulate immune responses. *J. Cell. Immunother.* **2016**, *2*, 1–10.

43. Hompland, T.; Ellingsen, C.; Øvrebø, K. M.; Rofstad, E. K. Interstitial fluid pressure and associated lymph node metastasis revealed in tumors by dynamic contrast-enhanced MRI. *Cancer Res.* **2012**, *72*, 4899–4908.

44. Fan, Y.; Du, W.; He, B.; Fu, F.; Yuan, L.; Wu, H.; Dai, W.; Zhang, H.; Wang, X.; Wang, J.; Zhang, X.; Zhang, Q. The reduction of tumor interstitial fluid pressure by liposomal imatinib and its effect on combination therapy with liposomal doxorubicin. *Biomaterials* **2013**, *34*, 2277–2288.

45. Lubberink, M.; Golla, S. S. V; Jonasson, M.; Rubin, K.; Glimelius, B.; Sorensen, J.; Nygren, P. (15)O-Water PET Study of the Effect of Imatinib, a Selective Platelet-Derived Growth Factor Receptor Inhibitor, Versus Anakinra, an IL-1R Antagonist, on Water-Perfusable Tissue Fraction in Colorectal Cancer Metastases. *J. Nucl. Med.* **2015**, *56*, 1144–1149.

46. Wagstaff, K.; Jans, D. Protein Transduction: Cell Penetrating Peptides and Their Therapeutic Applications. *Curr. Med. Chem.* **2006**, *13*, 1371–1387.

47. Liu, J. N.; Bu, W.; Pan, L. M.; Zhang, S.; Chen, F.; Zhou, L.; Zhao, K. Le; Peng, W.; Shi, J. Simultaneous nuclear imaging and intranuclear drug delivery by nuclear-targeted multifunctional upconversion nanoprobes. *Biomaterials* **2012**, *33*, 7282–7290.

48. Zheng, X. T.; Ma, X. Q.; Li, C. M. Highly efficient nuclear delivery of anti-cancer drugs using a bio-functionalized reduced graphene oxide. *J. Colloid Interface Sci.* **2016**, *467*, 35–42.

49. Kumar, B.; Kulanthaivel, S.; Mondal, A.; Mishra, S.; Banerjee, B.; Bhaumik, A.; Banerjee, I.; Giri, S. Mesoporous silica nanoparticle based enzyme responsive system for colon specific drug delivery through guar gum capping. *Colloids Surfaces B Biointerfaces* **2016**, *150*, 352–361.

50. Pan, L.; He, Q.; Liu, J.; Chen, Y.; Ma, M.; Zhang, L.; Shi, J. Nuclear-Targeted Drug Delivery of TAT Peptide-Conjugated Monodisperse Mesoporous Silica Nanoparticles. *J. Am. Chem. Soc.* **2012**, *134*, 5722–5725.

51. Xiao, Q.; Zheng, X.; Bu, W.; Ge, W.; Zhang, S.; Chen, F.; Xing, H.; Ren, Q.; Fan, W.; Zhao, K.; Hua, Y.; Shi, J. A Core/Satellite Multifunctional Nanotheranostic for *in vivo* Imaging and Tumor Eradication by Radiation/Photothermal Synergistic Therapy. *J. Am. Chem. Soc.* **2013**, *135*, 13041–13048.

52. Louie, A. Multimodality imaging probes: Design and challenges. *Chem. Rev.* **2010**, *110*, 3146–3195.

53. Lu, J.; Liong, M.; Li, Z.; Zink, J. I.; Tamanoi, F. Biocompatibility, Biodistribution, and Drug-Delivery Efficiency of Mesoporous Silica Nanoparticles for Cancer Therapy in Animals. *Small* **2010**, *6*, 1794–1805.

54. Veiseh, O.; Gunn, J. W.; Zhang, M. Design and fabrication of magnetic nanoparticles for targeted drug delivery and imaging. *Adv. Drug Deliv. Rev.* **2010**, *62*, 284–304.

55. Reddy, G. R.; Bhojani, M. S.; McConville, P.; Moody, J.; Moffat, B. A.; Hall, D. E.; Kim, G.; Koo, Y. E. L.; Woolliscroft, M. J.; Sugai, J. V.; Johnson, T. D.; Philbert, M. A.; Kopelman, R.; Rehemtulla, A.; Ross, B. D. Vascular targeted nanoparticles for imaging and treatment of brain tumors. *Clin. Cancer Res.* **2006**, *12*, 6677–6686.

56. Schmieder, A. H.; Caruthers, S. D.; Zhang, H.; Williams, T. A.; Robertson, J. D.; Wickline, S. A.; Lanza, G. M. Three-dimensional MR mapping of angiogenesis with alpha5beta1(alpha nu beta3)-targeted theranostic nanoparticles in the MDA-MB-435 xenograft mouse model. *Faseb J* **2008**, *22*, 4179–4189.

57. Grange, C.; Geninatti-Crich, S.; Esposito, G.; Alberti, D.; Tei, L.; Bussolati, B.; Aime, S.; Camussi, G. Combined delivery and magnetic resonance imaging of neural cell adhesion molecule-targeted doxorubicin-containing liposomes in experimentally induced Kaposi's sarcoma. *Cancer Res.* **2010**, *70*, 2180–2190.

58. Cittadino, E.; Ferraretto, M.; Torres, E.; Maiocchi, A.; Crielaard, B. J.; Lammers, T.; Storm, G.; Aime, S.; Terreno, E. MRI evaluation of the antitumor activity of paramagnetic liposomes loaded with prednisolone phosphate. *Eur. J. Pharm. Sci.* **2012**, *45*, 436–441.

59. Nanoparticles, F. M.; Enhanced, M.; Imaging, C.; Subjects, L. Fluorescent Magnetic Nanoparticles for Magnetically Enhanced Cancer Imaging and Targeting in Living. **2012**, 6862–6869.

60. Gaykema, S. B. M.; Brouwers, A. H.; Lub-de Hooge, M. N.; Pleijhuis, R. G.; Timmer-Bosscha, H.; Pot, L.; van Dam, G. M.; van der Meulen, S. B.; de Jong, J. R.; Bart, J.; de Vries, J.; Jansen, L.; de Vries, E. G. E.; Schröder, C. P. 89Zr-Bevacizumab PET Imaging in Primary Breast Cancer. *J. Nucl. Med.* **2013**, *54*, 1–5.

61. Haubner, R.; Beer, A. J.; Chen, X. NIH Public Access. **2013**, *37*, 1–29.

62. Ferrara, N. Vascular endothelial growth factor. *Arterioscler. Thromb. Vasc. Biol.* **2009**, *29*, 789–791.

63. Tijink, B. M.; Perk, L. R.; Budde, M.; Stigter-Van Walsum, M.; Visser, G. W. M.; Kloet, R. W.; Dinkelborg, L. M.; Leemans, C. R.; Neri, D.; Van Dongen, G. A. M. S. 124I-L19-SIP for immuno-PET imaging of tumour vasculature and guidance of 131I-L19-SIP radioimmunotherapy. *Eur. J. Nucl. Med. Mol. Imaging* **2009**, *36*, 1235–1244.

64. Birchler, M. T.; Thuerl, C.; Schmid, D.; Neri, D.; Waibel, R.; Schubiger, A.; Stoeckli, S. J.; Schmid, S.; Goerres, G. W. Immunoscintigraphy of patients with head and neck carcinomas, with an anti-angiogenetic antibody fragment. *Otolaryngol. - Head Neck Surg.* **2007**, *136*, 543–548.

65. Levashova, Z.; Backer, M.; Backer, J. M.; Blankenberg, F. G. Imaging vascular endothelial growth factor (VEGF) receptors in turpentine-induced sterile thigh abscesses with radiolabeled single-chain VEGF. *J Nucl Med* **2009**, *50*, 2058–2063.

66. Leung, K. Biotinylated vascular endothelial growth factor121-Avi-streptavidin-IRDye800 2004.

67. Shayan, R.; Achen, M. G.; Stacker, S. A. Lymphatic vessels in cancer metastasis: bridging the gaps. *Carcinogenesis* **2006**, *27*, 1729–1738.

68. Yang, H.; Zou, L. G.; Zhang, S.; Gong, M. F.; Zhang, D.; Qi, Y. Y.; Zhou, S. W.; Diao, X. W. Feasibility of MR imaging in evaluating breast cancer lymphangiogenesis using Polyethylene glycol-GoldMag nanoparticles. *Clin. Radiol.* **2013**, *68*, 1233–1240.

69. Sun, L.; Wu, Q.; Peng, F.; Liu, L.; Gong, C. Strategies of polymeric nanoparticles for enhanced internalization in cancer therapy. *Colloids Surfaces B Biointerfaces* **2015**, *135*, 56–72.

70. Luo, G.; Yu, X.; Jin, C.; Yang, F.; Fu, D.; Long, J.; Xu, J.; Zhan, C.; Lu, W. LyP-1-conjugated nanoparticles for targeting drug delivery to lymphatic metastatic tumors. *Int. J. Pharm.* **2010**, *385*, 150–156.

71. Zhang, F.; Niu, G.; Lin, X.; Jacobson, O.; Ma, Y.; Eden, H. S.; He, Y.; Lu, G.; Chen, X. Imaging tumor-induced sentinel lymph node lymphangiogenesis with LyP-1 peptide. *Amino Acids* **2012**, *42*, 2343–2351.

72. Wang, Z.; Yu, Y.; Ma, J.; Zhang, H.; Zhang, H.; Wang, X.; Wang, J.; Zhang, X.; Zhang, Q. LyP-1 modification to enhance delivery of artemisinin or fluorescent probe loaded polymeric micelles to highly metastatic tumor and its lymphatics. *Mol. Pharm.* **2012**, *9*, 2646–2657.

73. Peer, D.; Margalit, R. Loading mitomycin C inside long circulating hyaluronan targeted nano-liposomes increases its antitumor activity in three mice tumor models. *Int. J. Cancer* **2004**, *108*, 780–789.

74. Kanapathipillai, M.; Mammoto, A.; Mammoto, T.; Kang, J. H.; Jiang, E.; Ghosh, K.; Korin, N.; Gibbs, A.; Mannix, R.; Ingber, D. E. Inhibition of mammary tumor growth using lysyl oxidase-targeting nanoparticles to modify extracellular matrix. *Nano Lett.* **2012**, *12*, 3213–3217.

75. Wang, Y.; Lin, T.; Zhang, W.; Jiang, Y.; Jin, H.; He, H.; Yang, V. C.; Chen, Y.; Huang, Y. A prodrug-type, MMP-2-targeting nanoprobe for tumor detection and imaging. *Theranostics* **2015**, *5*, 787–795.

76. Schuerle, S.; Dudani, J. S.; Christiansen, M. G.; Anikeeva, P.; Bhatia, S. N. Magnetically Actuated Protease Sensors for *in vivo* Tumor Profiling. *Nano Lett.* **2016**, *16*, 6303–6310.

77. Li, Y.; Foss, C. A.; Summerfield, D. D.; Doyle, J. J.; Torok, C. M.; Dietz, H. C.; Pomper, M. G.; Yu, S. M. Targeting collagen strands by photo-triggered triple-helix hybridization. **2012**.

78. Mao, Y.; Keller, E. T.; Garfield, D. H.; Shen, K.; Wang, J. Stromal cells in tumor microenvironment and breast cancer. *Cancer Metastasis Rev.* **2013**, *32*, 303–315.

79. Mantovani, A.; Bottazzi, B.; Colotta, F.; Sozzani, S.; Ruco, L. The origin and function of tumor-associated macrophages. *Immunol. Today* **1992**, *13*, 265–270.

80. Zhu, S.; Niu, M.; O'Mary, H.; Cui, Z. Targeting of tumor-associated macrophages made possible by PEG-sheddable, mannose-modified nanoparticles. *Mol. Pharm.* **2013**, *10*, 3525–3530.

81. Östman, A.; Augsten, M. Cancer-associated fibroblasts and tumor growth--bystanders turning into key players. *Curr. Opin. Genet. Dev.* **2009**, *19*, 67–73.

82. Kalluri, R.; Zeisberg, M. Fibroblasts in cancer. *Nat. Rev. Cancer* **2006**, *6*, 392–401.

83. Aggarwal, S.; Brennen, W. N.; Kole, T. P.; Schneider, E.; Topaloglu, O.; Yates, M.; Cotter, R. J.; Denmeade, S. R. Fibroblast activation protein peptide substrates identified from human collagen I

derived gelatin cleavage sites. *Biochemistry* **2008**, *47*, 1076–1086.

84. Loeffler, M.; Krüger, J. A.; Niethammer, A. G.; Reisfeld, R. A. Targeting tumor-associated fibroblasts improves cancer chemotherapy by increasing intratumoral drug uptake. *J. Clin. Invest.* **2006**, *116*, 1955–1962.

85. Miao, L.; Huang, L. Exploring the tumor microenvironment with nanoparticles. In *Nanotechnology-Based Precision Tools for the Detection and Treatment of Cancer*; Springer, 2015; pp. 193–226.

86. Milner, J. M.; Patel, A.; Rowan, A. D. Emerging roles of serine proteinases in tissue turnover in arthritis. *Arthritis Rheum.* **2008**, *58*, 3644–3656.

87. Kennedy, A.; Dong, H.; Chen, D.; Chen, W.-T. Elevation of seprase expression and promotion of an invasive phenotype by collagenous matrices in ovarian tumor cells. *Int. J. cancer* **2009**, *124*, 27–35.

88. Brennen, W. N.; Isaacs, J. T.; Denmeade, S. R. Rationale behind targeting fibroblast activation protein--expressing carcinoma-associated fibroblasts as a novel chemotherapeutic strategy. *Mol. Cancer Ther.* **2012**, *11*, 257–266.

89. Ji, T.; Zhao, Y.; Wang, J.; Zheng, X.; Tian, Y.; Zhao, Y.; Nie, G. Tumor Fibroblast Specific Activation of a Hybrid Ferritin Nanocage-Based Optical Probe for Tumor Microenvironment Imaging. *Small* **2013**, *9*, 2427–2431.

90. Ji, T.; Zhao, Y.; Ding, Y.; Wang, J.; Zhao, R.; Lang, J.; Qin, H.; Liu, X.; Shi, J.; Tao, N.; others Transformable Peptide Nanocarriers for Expeditious Drug Release and Effective Cancer Therapy via Cancer-Associated Fibroblast Activation. *Angew. Chemie* **2016**, *128*, 1062–1067.

91. Gondi, C. S.; Rao, J. S. Cathepsin B as a cancer target. *Expert Opin. Ther. Targets* **2013**, *17*, 281–291.

92. Victor, B. C.; Anbalagan, A.; Mohamed, M. M.; Sloane, B. F.; Cavallo-Medved, D. Inhibition of cathepsin B activity attenuates extracellular matrix degradation and inflammatory breast cancer invasion. *Breast Cancer Res.* **2011**, *13*, R115.

93. Mikhaylov, G.; Klimpel, D.; Schaschke, N.; Mikac, U.; Vizovisek, M.; Fonovic, M.; Turk, V.; Turk, B.; Vasiljeva, O. Selective targeting of tumor and stromal cells by a nanocarrier system displaying lipidated cathepsin b inhibitor. *Angew. Chemie Int. Ed.* **2014**, *53*, 10077–10081.

94. Mantovani, A.; Sozzani, S.; Locati, M.; Allavena, P.; Sica, A. Macrophage polarization: tumor-associated macrophages as a paradigm for polarized M2 mononuclear phagocytes. *Trends Immunol.* **2002**, *23*, 549–555.

95. Weissleder, R.; Nahrendorf, M.; Pittet, M. J. Imaging macrophages with nanoparticles. *Nat. Mater.* **2014**, *13*, 125–138.

96. Ries, C. H.; Cannarile, M. A.; Hoves, S.; Benz, J.; Wartha, K.; Runza, V.; Rey-Giraud, F.; Pradel, L. P.; Feuerhake, F.; Klaman, I.; others Targeting tumor-associated macrophages with anti-CSF-1R antibody reveals a strategy for cancer therapy. *Cancer Cell* **2014**, *25*, 846–859.

97. Collingridge, D. R.; Carroll, V. A.; Glaser, M.; Aboagye, E. O.; Osman, S.; Hutchinson, O. C.; Barthel, H.; Luthra, S. K.; Brady, F.; Bicknell, R.; Price, P.; Harris, A. L. The development of [124I]iodinated-VG76e: A novel tracer for imaging vascular endothelial growth factor *in vivo* using

positron emission tomography. *Cancer Res.* **2002**, *62*, 5912–5919.

98. Kang, C. M.; Koo, H.-J.; Lee, K. C.; Choe, Y. S.; Choi, J. Y.; Lee, K.-H.; Kim, B.-T. A vascular endothelial growth factor 121 (VEGF 121)-based dual PET/optical probe for *in vivo* imaging of VEGF receptor expression. *Biomaterials* **2013**, *34*, 6839–6845.

99. Badalà, F.; Nouri-mahdavi, K.; Raoof, D. A. NIH Public Access. *Computer (Long. Beach. Calif).* **2008**, *144*, 724–732.

100. Van Sluis, R.; Bhujwalla, Z. M.; Raghunand, N.; Ballesteros, P.; Alvarez, J.; Cerdán, S.; Galons, J. P.; Gillies, R. J. *In vivo* imaging of extracellular pH using 1H MRSI. *Magn. Reson. Med.* **1999**, *41*, 743–750.

101. Melancon, M. P.; Stafford, R. J.; Li, C. Challenges to effective cancer nanotheranostics. *J. Control. Release* **2012**, *164*, 177–182.

102. Fernandez-Fernandez, A.; Manchanda, R.; McGoron, A. J. Theranostic Applications of Nanomaterials in Cancer: Drug Delivery, Image-Guided Therapy, and Multifunctional Platforms. *Appl. Biochem. Biotechnol.* **2011**, *165*, 1628–1651.

103. Gobbo, O. L.; Sjaastad, K.; Radomski, M. W.; Volkov, Y.; Prina-Mello, A. Magnetic Nanoparticles in Cancer Theranostics. *Theranostics* **2015**, *5*, 1249–1263.

104. Shi, J.; Kantoff, P. W.; Wooster, R.; Farokhzad, O. C. Cancer nanomedicine: progress, challenges and opportunities. *Nat. Publ. Gr.* **2016**, *17*, 20–37.

105. Meyers, J. D.; Doane, T.; Burda, C.; Basilion, J. P. Nanoparticles for imaging and treating brain cancer. *Nanomedicine (Lond).* **2013**, *8*, 123–143.

106. Hu, Q.; Katti, P. S.; Gu, Z.; Hill, C.; Hill, C. HHS Public Access. **2015**, *6*, 12273–12286.

107. Sukumar, U. K.; Bhushan, B.; Dubey, P.; Matai, I.; Sachdev, A.; Packirisamy, G. Emerging Applications of Nanoparticles for Lung Cancer Diagnosis and Therapy. *Int Nano Lett* **2013**, *3*, 1–17.